Effects of Argon Dilution on the Translational and Rotational Temperatures of SiH in Silane and Disilane Plasmas

Jie Zhou, Jianming Zhang, and Ellen R. Fisher*

Department of Chemistry, Colorado State University, Fort Collins, Colorado 80523-1872

Received: July 26, 2005; In Final Form: September 27, 2005

The effects of argon dilution on the translational and rotational temperatures of SiH in both silane and disilane plasmas have been investigated using the imaging of radicals interacting with surfaces (IRIS) technique. The average rotational temperature of SiH determined from the SiH excitation spectra is ∼500 K in both SiH_4/Ar and Si_2H_6/Ar plasmas, with no obvious dependence on the fraction of argon dilution. Modeling of kinetic data yields average SiH translational temperatures of ∼1000 K, with no dependence on the fraction of argon in the SiH_4/Ar plasmas within the studied range. In the Si_2H_6/Ar plasmas, however, the translational temperature decreases from ∼1000 to ∼550 K as the Ar fraction in the plasma increases. Thus, at the highest Ar fractions, the translational and rotational temperatures are nearly identical, indicating that the SiH radicals are thermally equilibrated. The underlying chemistry and mechanisms of SiH energy equilibration in Ar-diluted plasmas are discussed.

I. Introduction

Silane and disilane plasmas have been extensively applied to the deposition of hydrogenated amorphous silicon films (α-Si:H). These materials are widely used in microelectronic devices such as solar cells, thin film transistors, and flat panel displays.[1−6] During the deposition processes, neutral SiH_x ($x = 0-3$) species are considered as important precursors for film growth.[1,7,8] Among these, the long-lived SiH_3 is considered the primary precursor for film growth, although the short-lived Si, SiH, and SiH_2 still have significant influence on film properties.[3,9,10] Investigations of the surface interactions of these species are, therefore, of practical importance to the improvement of film characteristics.

Chemically active radicals can be easily created in low-temperature plasmas through electron impact dissociation of precursor molecules. This is primarily because electrons in these systems have relatively high temperatures (10^3-10^5 K) in comparison to the gas temperature ($<10^3$ K).[11] The precursor fragments can obtain different kinetic energies during the dissipation of excess energy as a result of differences in mass as well as energy transfer pathways. Therefore, knowledge of the energy partitioning among these species is a key component of the plasma chemistry occurring during film growth. In most silane or disilane plasmas, however, the SiH density is low due to its high gas-phase reactivity and surface-sticking probability.[1,2,12,13]

SiH in plasma systems can be examined using various gas-phase diagnostics. For example, laser-induced fluorescence (LIF) is a sensitive plasma diagnostic tool that has been used extensively to investigate the nature of a variety of plasma species, including the SiH radical. Data on relative or absolute gas-phase concentrations, gas and surface reactivity, and kinetic energy have all been obtained with LIF.[2,11,14,15] Combining LIF and plasma molecular beam technology, our imaging of radicals interacting with surfaces (IRIS) technique is particularly useful and versatile. IRIS can provide spatially and temporally resolved 2-D images of plasma species of interest, and it has been applied to measure the surface interactions and translational/rotational temperatures of probed species.[16−18]

Previously, we have measured the surface interactions as well as the rotational (Θ_R) and translational temperatures (Θ_T) for SiH radicals in 100% silane and disilane plasmas as a function of applied rf power (P).[1,19] The SiH surface reactivity is near unity under all plasma conditions, showing no clear dependence on P, substrate temperature (T_S), and precursor gas. In addition, the average SiH rotational and translational temperatures were also independent of P and precursor gas, and they were measured as ∼600 and ∼1100 K for silane and disilane plasmas, respectively.[1] This difference between Θ_R and Θ_T indicates that SiH radicals are not in thermal equilibrium within the plasmas. A similar observation has also been made for OH in alkoxysilane/O_2 plasmas, wherein Θ_T(OH) is significantly higher than Θ_R(OH), again indicating a non thermalized system.[20−23] However, Θ_R and Θ_T for OH are nearly identical in H_2O plasmas, suggesting that OH radicals are in thermal equilibrium in this system.[21,23] These results led us to hypothesize that radicals produced by unimolecular dissociation processes (such as in the H_2O system) are more likely to reach thermal equilibrium than molecules formed via bimolecular reactions, such as in the alkoxysilane/O_2 systems.

The SiH results, however, would appear to disagree with this hypothesis, provided that SiH was formed through a stepwise dissociation process. Previously, we noted that SiH is formed by the direct electron-induced dissociation of SiH_4, rather than via sequential dissociation of SiH_3 or SiH_2.[1] Because this dissociation pathway proceeds via a super-excited electronic transition state, this creation mechanism may result in the significant differences measured in the rotational and translational temperatures of SiH. Moreover, the extremely high gas-phase reactivity of SiH may also contribute to this discrepancy. Specifically, SiH is very reactive with SiH_4, such that the SiH radicals probed in the molecular beam are mainly produced close to the extraction orifice, and have undergone only ∼5 collisions

* Author to whom correspondence should be addressed. E-mail: erfisher@lamar.colostate.edu.

10.1021/jp0541213 CCC: $30.25
Published on Web 11/02/2005

prior to exiting the reactor. Thus, there are not enough collisions to allow SiH to reach thermal equilibrium. One can expect that the discrepancy between Θ_R and Θ_T of SiH can be reduced or eliminated if there are more nonreactive collisions for SiH. Therefore, we have investigated the effects of argon dilution on Θ_T and Θ_R of SiH in both silane and disilane plasmas. The argon dilution in these systems can provide additional nonreactive-collisional cooling for SiH, as well as more information on the energetics characterization of reactive plasma species. The process of thermal equilibration of SiH radicals is also discussed.

II. Experiment

The rotational and translational temperatures of SiH have been measured with our IRIS apparatus, which has been described in detail previously.[1,20,24] Briefly, the precursor gases enter at the rear of a tubular glass reactor, rf power (13.56 MHz, Advanced Energy) is applied to an inductor coil, and a plasma is produced. For the SiH_4/Ar and Si_2H_6/Ar mixtures, the total flow rates are maintained at 20 and 15 sccm, respectively, which leads to source pressures of 35−50 mTorr. The plasma expands through a 9.5-mm diameter orifice and a series of collimating slits (∼1 mm) and enters a differentially pumped region; to reach the interaction chamber, the beam then passes through a series of collimating slits (∼1-mm wide) into a high-vacuum chamber. The typical pressure in the differential chamber is maintained below 10^{-5} Torr during experiments, and that in the main chamber is $\sim 10^{-6}-10^{-5}$ Torr. The mean free path of SiH molecules in the plasma reactor is ∼1 mm. Because the collimating slit widths are ∼1 mm, the molecular beam can be classified as collisionless and "near effusive".[1,19,25] This is discussed further below.

An excimer-pumped tunable dye laser (XeCl, Lambda Physik LPX210I, Scanmate2) beam intersects the plasma molecular beam at a 90° angle downstream from the source and excites the ground-state SiH radicals in the plasma molecular beam, resulting in LIF signals. The spatially and temporally resolved LIF images were collected by an electronically gated and intensified charge-coupled device (ICCD), located perpendicular to both the laser and plasma molecular beams, directly above the interaction region.

Silane (Voltaix, 99.999%), disilane (Voltaix, 99.99%), and argon (Air Products, 99.999%) were used as feed gases. For mixture gases, the fraction of SiH_4 or Si_2H_6 is defined as the ratio of the flow rate of SiH_4 or Si_2H_6 to the flow rate of Ar. For all experiments, the applied rf power was 60 W, and the total pressure in the source was 50 mTorr, regardless of the flow rates used. Exalite 417 dye (Exciton) was used in the dye laser to probe the SiH $A^2\Delta-X^2\Pi$ transition. The output laser energy with this dye was typically 3−7 mJ/pulse. Rotational lines Q_1 ($J = 10.5$) at 413.418 nm and R_2 ($J = 2.5$) at 413.428 nm were used for the rotational temperature measurements because the relatively large difference in rotational quantum number means the relationship between these two peaks is sensitive to Θ_R. The R_{12} ($J = 1.5$) rotational line at 414.438 nm was used for translational temperature measurements because of its higher LIF intensity. Measurements of the SiH LIF signal intensity as a function of laser energy yielded typical optical saturation behavior. All measurements were performed with the laser energy in the optical saturation regime such that the data were not affected by small fluctuations in laser power.

The rotational temperature of SiH was measured by collecting SiH fluorescence excitation spectra with the ICCD images 4 × 4 binned to increase the signal-to-noise ratio. The gate delay and gate width of the ICCD camera were set at 205 and 2000 ns, respectively. These settings allow for the collection of fluorescence over the entire radiative lifetime of the SiH $A^2\Delta$ state (534 ns).[26] The scan range was from 413.40 to 413.45 nm with 0.001-nm steps and 1500 laser shots per step. The rotational temperature of SiH is determined from simulations of the Q_1 ($J = 10.5$) and R_2 ($J = 2.5$) rotational lines using the LIFBASE program[27] at different temperatures until a best fit to the experimental data is obtained.

Four different gate delays, typically 205, 505, 805, and 1105 ns after the laser pulse, and a relatively short gate width of 100 ns were used for SiH velocity measurements. The pixels on the ICCD were not binned for the velocity measurements, yielding the highest spatial resolution and thus the most accurate measurement of the molecules' movement. The CCD camera has a resolution of 0.1008 mm/pixel for velocity measurements. The LIF signals were collected for 8 or 12 accumulations of 10^4 laser shots at each time delay. Cross sections of the LIF images along the molecular beam were obtained by averaging 100 rows of pixels in the laser beam axis. To accurately determine the peak position of LIF intensity, a symmetrical laser spatial profile is assumed and the cross section is fit by a Gaussian function. The SiH velocity then can be calculated from the spatial shift in the maximum fluorescence intensity at the four time delays by plotting them as a function of time delay and fitting with a linear regression analysis.[1,16] The slope of this linear fit gives the average velocity of SiH along the center axis of the molecular beam. The average velocity obtained by this method represents a lower limit to the translational velocity of SiH because the molecules in the molecular beam also move in the radial directions. Thus, a Monte Carlo simulation program was used to calculate the cross section of the spatial LIF intensity as a function of time delay at different Θ_T.[18] This simulation assumes that the velocity distribution of SiH in the bulk plasma can be described by a Maxwell−Boltzmann distribution. The peak positions of simulated cross sections are then analyzed as described above for the experimental data. Comparison of the experimentally obtained value with the simulated values is performed in an iterative manner, yielding the velocity of the SiH in the plasma. The translational temperature can then be calculated from the velocity distribution, ($\Theta_T = \pi m v^2/8k$, where m is the mass of the radical and k is Boltzmann constant).[1] This method is sensitive to small spatial shifts, which works well for species with relatively short fluorescence lifetimes because a limited range of time delays can be used.

III. Results

Figure 1 shows the 2-D ICCD images of SiH LIF signals using a 100% Si_2H_6 plasma molecular beam ($P = 60$ W) at gate delays of 205, 505, 805, and 1105 ns. In these images, the plasma molecular beam moves from left to right and the laser is propagating from bottom to top. As the gate delay increases, the SiH LIF intensity decreases significantly due to the radiative decay of the excited SiH $A^2\Delta$ state after laser excitation.[1] Figure 2a shows the corresponding x-cross sections of the SiH LIF images in Figure 1. For the shortest time interval, we observe a peak position shift of ∼0.2 mm. Although the shifts of the maximum LIF intensity along the direction of the molecular beam can be seen in the cross sections, they are better distinguished when plotted as a function of time delay, as in the inset of Figure 2a. The linear regression analysis yields a slope of 759 m/s, which represents a lower limit to the average SiH velocity in the molecular beam. This value corresponds to $\Theta_T(\mathrm{SiH}) = 789$ K. To obtain a more accurate average velocity

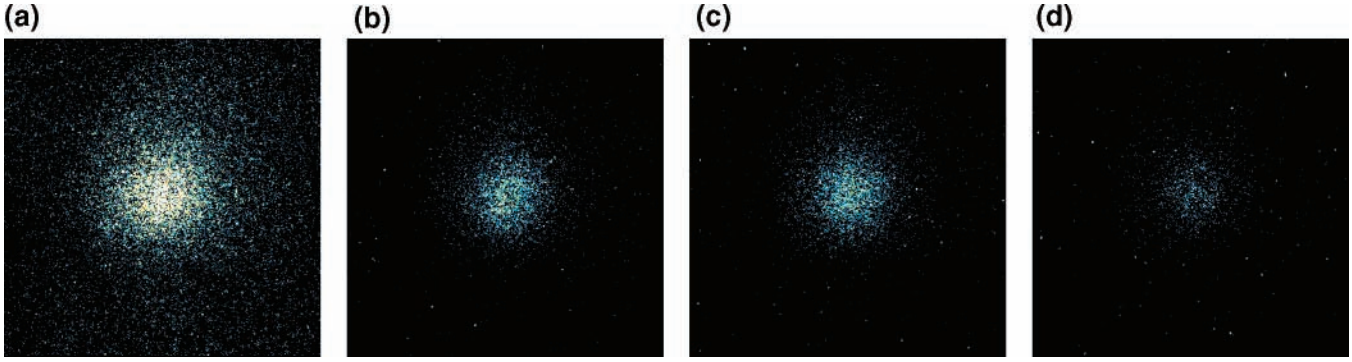

Figure 1. ICCD images of LIF signals for SiH radicals in a 100% Si_2H_6 plasma molecular beam ($P = 60$ W) at four different gate delays: (a) 205 ns, (b) 505 ns, (c) 805 ns, and (d) 1105 ns after laser excitation. The intensity scales in (a) and (b) are identical; due to the lower signal intensity in (c) and (d), the data have been multiplied by a factor of 2.

and the corresponding average translational temperature, the spatial shifts as a function of time delay have been simulated at different translational temperatures until a good agreement between the experimental and simulated results is obtained. The simulation results are also plotted in Figure 2a, yielding an average kinetic velocity of 760 ± 62 m/s and corresponding average translational temperature of $\Theta_T = 820 \pm 129$ K. The discrepancies between the model and the experimental signal shapes in Figure 2 are the result of the radial movement of the molecular beam in all directions during the expansion through a slit, resulting in "wings" on the data. For the velocity measurements, however, the peak positions are the critical dimension being simulated, and this is not significantly affected by the wider wings at lower delay times.

Figure 2b shows the cross-sectional plots of SiH LIF images for a mixed Si_2H_6/ Ar plasma with a 2:1 ratio (67% Si_2H_6). The cross sections and the corresponding linear regression analysis are very similar to those shown in Figure 2a. The slope of the linear regression fit is, however, somewhat lower than that for the 100% Si_2H_6 plasma, 607 m/s. The simulation yields a correspondingly lower Θ_T of 525 ± 96 K for the Ar-diluted system.

We have previously collected extensive excitation data for SiH over a wide range of wavelengths (411−414.5 nm)[1,19] and have measured the rotational temperature from these spectra. Here, we again collected excitation spectra over a reasonably wide wavelength range and found good agreement with these previous results. For the purposes of determining Θ_R in this work, we focused on two rotational lines with significantly different quantum states. Figure 3 shows the experimental and simulated excitation spectra of SiH $A^2\Delta - X^2\Pi$ from 413.40 to 413.45 nm collected using a 100% Si_2H_6 plasma molecular beam (Figure 3a) and a 67% Si_2H_6 plasma molecular beam (Figure 3b). These data clearly show that the populations of the two states are similar for the two different plasma conditions, although it appears that the $Q_1(J = 10.5)$ rotational state is slightly more populated in the diluted plasma system. As can be seen in Figure 3, excellent fits between the experimental and simulated data were obtained for both data sets. Because these two rotational lines have quite different J quantum numbers (10.5 and 2.5), the ratio of these two peaks heights will be sensitive to changes in the rotational temperatures. As noted above, we have previously fit larger portions of the rotational spectrum for SiH and find good correspondence between these fits and the fits to the two rotational states chosen for analysis in this study.[1,19] From several data sets, the simulation yielded a rotational temperature of 520 ± 10 K for

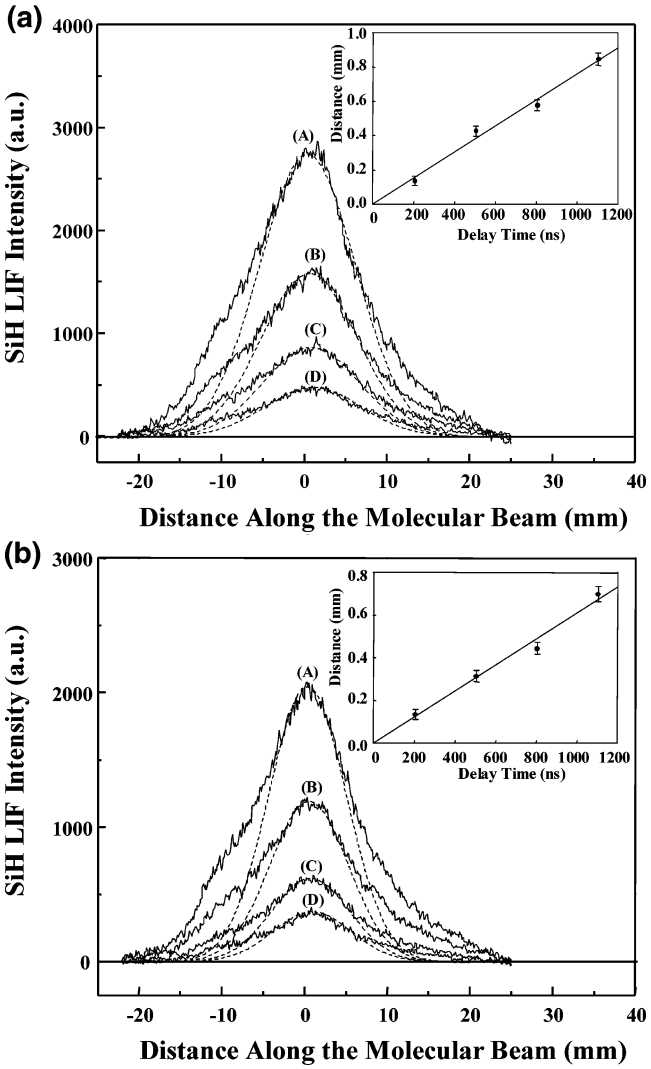

Figure 2. (a) Cross-sectional data for the SiH LIF images shown in Figure 1 (solid lines) at four different time delays: (A) 205 ns, (B) 505 ns, (C) 805 ns, and (D) 1105 ns after laser excitation. Simulated curves for $\Theta_T = 820$ K are also shown (dashed lines). In the inset, the spatial positions of the maxima of the LIF signals are plotted as a function of time delay. The slope of the linear regression analysis corresponds to the velocity (759 m/s) of the SiH radicals along the central axis of the molecular beam. (b) Cross-sectional data of SiH radicals in a 2:1 Si_2H_6/Ar plasma (67% Si_2H_6) at the same four gate delays, along with simulated curves for SiH with $\Theta_T = 525$ K.

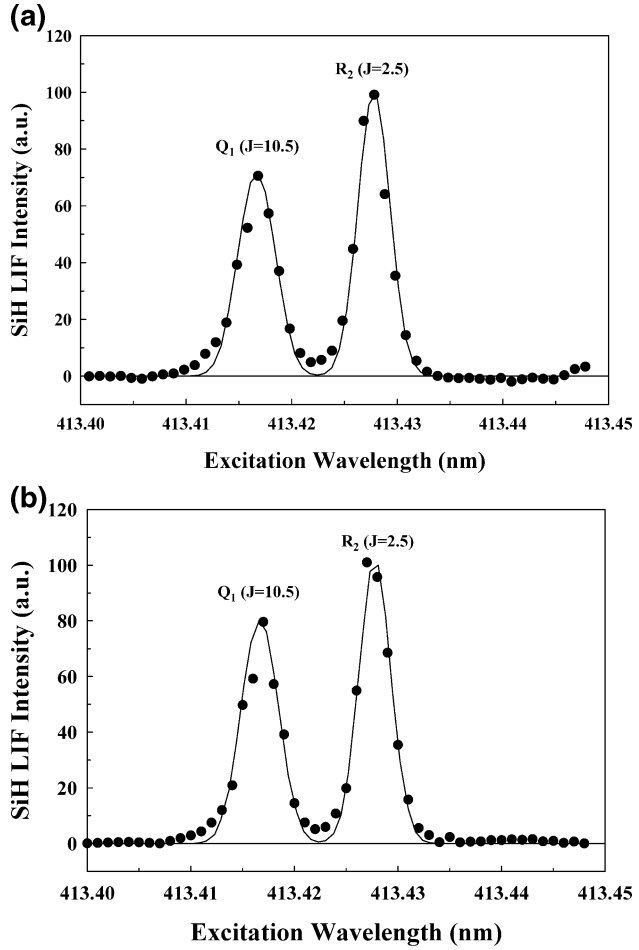

Figure 3. The SiH $A^2\Delta-X^2\Pi$ excitation spectra (solid circles) from 413.40 to 413.45 nm obtained in (a) a 100% Si_2H_6 plasma and (b) a 67% Si_2H_6 plasma. The simulated excitation spectra for each system using the LIFBASE program are also shown (solid lines). The best fits between the experimental and simulated data correspond to rotational temperatures of 520 K for the 100% Si_2H_6 plasma and 550 K for the 67% Si_2H_6 plasma.

the 100% Si_2H_6 data set and 550 ± 30 K for the 67% Si_2H_6 data set. These values are consistent with the observation that the $J = 10.5$ state is more highly populated in the diluted plasma system.

Figures 4 and 5 contain the average Θ_T and Θ_R values determined for SiH in SiH_4/Ar and Si_2H_6/Ar plasmas as a function of SiH_4 and Si_2H_6 fractions in the mixtures, respectively. As noted in the Experimental Section, the fraction of SiH_4 and Si_2H_6 in the mixture is defined as the ratio of the flow rate of SiH_4 or Si_2H_6 to the flow rate of Ar. For the rotational temperatures of SiH, no clear dependence on the argon dilution is found in either silane or disilane plasmas. The weighted average Θ_R values for SiH in SiH_4/Ar and Si_2H_6/Ar plasmas (averaging all dilution conditions) are 490 ± 10 K and 530 ± 10 K, respectively. In contrast, Θ_T for SiH demonstrates different trends in the two plasma systems. No significant dependence on Ar dilution is seen in the SiH_4/Ar plasma within the investigated fraction range of SiH_4 from 0.5 to 1.0, as shown in Figure 4. At lower SiH_4 fractions, the SiH signal decreases to below the detectable limit in our apparatus. In the Si_2H_6/Ar plasma, however, the translational temperature of SiH increases significantly with increasing Si_2H_6 fraction. When the fraction of Si_2H_6 reaches 0.67, the translational temperature of SiH is almost equal to its rotational temperature, which indicates that SiH radicals reach thermal equilibrium in this plasma system.

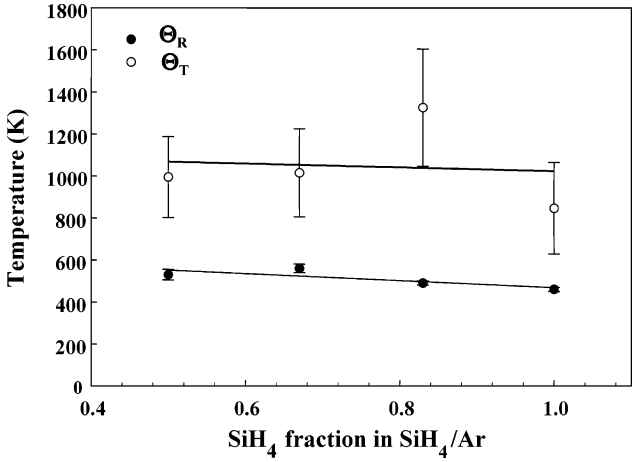

Figure 4. The average translational (open circles) and rotational (solid circles) temperatures of SiH radicals in SiH_4/Ar plasmas as a function of SiH_4 fraction in the feed gas. The lines are linear regression fits to the data.

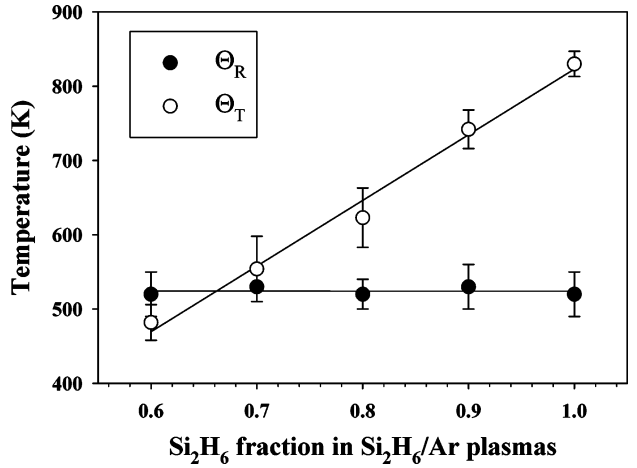

Figure 5. The average translational (open circles) and rotational (solid circles) temperatures of SiH radicals in Si_2H_6/Ar plasmas as a function of the Si_2H_6 fraction in the feed gas. The lines are linear regression fits to the data.

IV. Discussion

The energy distribution of radicals produced in a plasma system largely depends on their formation mechanisms. In silane and disilane plasmas, the primary radical fragments formed through direct electron impact reactions are quite different. The primary radicals produced in the SiH_4 plasma are given in reactions 1−4,[8,10,14,15,28−30] where the numbers in parentheses refer to the fraction of the radicals in the gas phase:

$$SiH_4 + e \rightarrow SiH_3\ (0.830) + H \quad (1)$$

$$SiH_4 + e \rightarrow SiH_2\ (0.097) + H_2 \quad (2)$$

$$SiH_4 + e \rightarrow SiH\ (0.047) + H_2 + H \quad (3)$$

$$SiH_4 + e \rightarrow Si\ (0.026) + 2H_2 \quad (4)$$

Note that the production mechanisms for SiH radicals have been studied extensively. From these works, it is commonly accepted that SiH radicals are formed primarily from the direct electron impact dissociation of SiH_4, reaction 3.[1,10,14,29] In contrast, for Si_2H_6 plasma, SiH is not formed from the direct electron impact dissociation of Si_2H_6.[1,3,10] The primary Si_2H_6 dissociation reactions in Si_2H_6 plasmas are given in reactions 5−7:[3,10]

$$Si_2H_6 + e \rightarrow SiH_2 + SiH_4 \rightarrow SiH_2\,(0.300) + SiH_3\,(0.340) + H \quad (5)$$

$$Si_2H_6 + e \rightarrow Si_2H_5\,(0.340) + H \quad (6)$$

$$Si_2H_6 + e \rightarrow SiH_3SiH\,(0.020) + H_2 \quad (7)$$

In a disilane plasma, SiH radicals are mainly produced by further dissociation of the primary product SiH_4, presumably via reaction 3, or possibly by a stepwise dissociation mechanism (i.e., $SiH_4 \rightarrow SiH_3 \rightarrow SiH_2 \rightarrow SiH$).[1,3,10]

During the dissociation of precursor molecules via electron impact reactions, the released excess energy is transferred to the dissociated fragments. This can lead to a high initial translational and rotational energy for these fragments,[1,7,14−16] which can be dissipated through collisional cooling. The rotational temperatures of SiH in both silane and disilane plasmas are nearly the same at all gas ratios, indicating that the rotational energy of SiH has been thermally equilibrated. This is supported by the observation that the rotational relaxation rate of SiH is fairly high (1.5×10^{-10} cm^3/s),[31] such that the rotational temperature of SiH is likely thermalized to the average gas temperature before it is extracted from the plasma source. It is a common assumption that the rotational temperature of the gas-phase radicals is equal to the average ambient gas temperature because the high initial rotational energy can be easily dissipated through rotational−rotational and rotational−translational energy transfer due to the high rotational relaxation rate.[1,4,32] Thus, in our systems, we believe the gas temperature is ∼500 K, in good agreement with what we found previously for SiH_4 and Si_2H_6 plasmas over a range of applied rf powers ($P = 20-80$ W).[1]

It is also commonly accepted that the average rotational temperature of the gas-phase species in plasmas is equal to their average translational temperature and thus to the ambient gas temperature. Our results for SiH do not, however, support this assumption. Indeed, the Θ_T values measured for SiH in both SiH_4/Ar and Si_2H_6/Ar plasmas are significantly higher than the gas temperature (∼1000 K vs ∼500 K) under most dilution conditions. This indicates that the initially high translational energy has not been thermalized prior to extraction from the source. The observation that Θ_T is nearly the same as Θ_R at the highest Ar dilution for Si_2H_6 plasma is discussed further below.

One possibility for the significantly higher Θ_T values found in the SiH_4 systems and in most of the Si_2H_6 systems is that there has been some supersonic expansion in the molecular beam. For a typical supersonic expansion molecular beam, however, the internal energy of molecules is transferred to the kinetic energy during the expansion, leading to very low Θ_R values (e.g., <50 K). In our systems, $\Theta_R \sim 550$ K, significantly higher than typical supersonic beams. Moreover, if supersonic expansion was occurring, Θ_T would be high under all conditions and the addition of Ar would not affect these values (as the pressure is the same). For the most diluted Si_2H_6 plasmas, however, we measure a lower Θ_T for SiH, indicating that the dilution significantly affects the translational temperature, most likely through collisional cooling. One additional point can be made from previous results in our laboratory for a 100% H_2O plasma, wherein we measured the rotational and translational temperatures of OH radicals as nearly identical, with no dependence on applied rf power.[20] Finally, we have previously explicitly tested the effects of orifice size and find no dependence on this parameter for either the Θ_T or Θ_R for SiH radicals. Thus, we are confident that the effects we observe are not the result of supersonic expansion of our molecular beam.

Gas-phase production and loss reactions of radicals are important for understanding thermal equilibration processes in a plasma system. Like other highly reactive radicals such as Si and SiH_2, SiH easily reacts with SiH_4 via reaction 8:

$$SiH + SiH_4 \leftrightarrow Si_2H_5^* + M \rightarrow Si_2H_5 \quad (8)$$

where M is a third body that collisionally stabilizes Si_2H_5*.[33] Nomura et al. measured the rate constant of this reaction as 4.8×10^{-11} $cm^3\ mol^{-1}\ s^{-1}$ in the afterglow of an SiH_4/Ar plasma at 300 K.[33] Reaction 8 has, therefore, been considered as the primary gas-phase loss mechanism of SiH in silane plasmas.[9] As noted above, the primary creation mechanism for SiH is reaction 3 in both silane and disilane plasmas. Thus, the balance between these two processes affects both the SiH density in the plasma as well as the thermalization of the translational and internal energies. For example, the increase of Ar in both systems results in a significant decrease (∼factor of 2−3 at 30% Ar) in the number density of SiH as a result of fewer precursor molecules. Likewise, the translational temperature of SiH shows different trends as a function of argon dilution in SiH_4/Ar and Si_2H_6/Ar plasmas, as shown in Figures 4 and 5. In the Si_2H_6/Ar plasma, a clear dependence on the Ar fraction is found, whereas there is no dependence on Ar dilution in the SiH_4/Ar plasma. This difference in the translational temperatures indicates that SiH radicals in the silane and disilane plasmas have different thermal equilibration rates.

This can be understood by examining the source of the SiH being detected in the IRIS experiments. In the 100% silane and disilane plasmas, the loss rate of SiH radicals via reaction with SiH_4 is high due to the relatively high density of SiH_4. The detected SiH radicals in these systems must, therefore, be those extracted from the plasma reactor before their kinetic energy has been thermalized via nonreactive collisions with SiH_4. These SiH radicals have a relatively high translational energy of ∼1000 K, which arises from the initial dissociation processes. It is assumed that the third body collisional stabilization in process 8 comes primarily from precursor gas molecules in each system.

The gas-phase chemistry of the two systems is significantly affected by Ar dilution. Specifically, the dilution affects the density of SiH_4 in the SiH_4/Ar and Si_2H_6/Ar plasmas differently. In the disilane system, SiH radicals are produced via subsequent dissociation of SiH_4 that is formed via electron impact of Si_2H_6, reaction 5. Because this is a secondary dissociation pathway, the SiH_4 density is relative low, especially at high fractions of argon. SiH radicals formed in the disilane system are thus more likely to be thermalized via nonreactive collisions before they are lost through reaction with SiH_4. In the silane plasmas, however, the relative SiH_4 density is significantly higher than that in a disilane plasma. Thus, the loss of SiH via reaction with SiH_4 is high, even at argon fractions of 0.5. Hence, the SiH radicals detected within the investigated dilution range are most likely nascent SiH radicals formed via reaction 3, thereby maintaining a high translational energy, even with the addition of Ar.

Support for this hypothesis comes from literature studies of Si atoms and SiH_2 in SiH_4/Ar systems. In comparison, Si atoms have a much higher reactivity with SiH_4 than SiH,[9,34] whereas SiH_2 has a comparable reactivity to SiH.[33] Tanaka et al. measured the translational temperature of Si in a 50-mTorr SiH_4/Ar plasma using laser absorption spectroscopy.[34] From their data, Θ_T(Si) decreases significantly when the fraction of SiH_4 is lower than 0.5. In the 100% SiH_4 system, $\Theta_T(Si) \sim 680$ K,

whereas at 20% SiH_4, $\Theta_T(Si) \sim 480$ K. At 5% SiH_4, the translational temperature of Si reaches room temperature, which indicates that the Si radicals have been completely thermalized. In contrast, Kono et al. measured the translational temperature of SiH_2 in SiH_4/Ar plasmas (40 mTorr, 4.5 W) and found that $\Theta_T(SiH_2)$ is close to room temperature, 336 ± 34 K, regardless of the SiH_4 mixing ratio. Because of the high reactivity of atomic Si with SiH_4 molecules, Si atoms are lost via the Si + SiH_4 reaction before their kinetic energy is thermalized by nonreactive collisions with SiH_4 and Ar. For SiH_2, the rate constant of the SiH_2 + SiH_4 reaction is fairly large, but it is still an order of magnitude smaller than that of the Si + SiH_4 reaction. Thus, it is likely that SiH_2 produced via dissociation of SiH_4 can experience several nonreactive collisions before it is lost via the SiH_2 + SiH_4 reaction, even in pure SiH_4 plasma. This can explain the low and nearly constant translational temperature of SiH_2.

Although the reactions of Si atoms and SiH_2 molecules in SiH_4/Ar systems are not identical to our SiH systems, the trends are the same. The translational energy dissipation and equilibration of a species is determined by the nonreactive collisional rate. Species with lower reactivity in higher inert gas-diluted systems will have more efficient collisional cooling, thereby increasing the rate of thermal equilibration of translational energy.

One additional note about the effects of Ar dilution on the gas-phase chemistry in the plasmas is that the initial rotational, vibrational, and translational energy for species such as SiH originates from the dissociation process of the parent molecule, primarily via electron impact reactions. Thus, the initial energy obtained in these degrees of freedom is associated with the electron energy in the plasmas. Although we have not explicitly measured the electron energy in the silane systems, we have previously measured it in similar CH_4/Ar plasmas,[35] and found there is little variation in the electron energy with Ar addition when the plasma is in an inductively coupled regime. Hence, we assume there is little variation in electron energy in the present systems. Nonetheless, even small variations could result in differences in the initial rotational, vibrational, and translational energy distribution, which may be altered as the result of thermalizing collisions in the plasma. We have explicitly demonstrated the effects of thermalizing collisions on Θ_T and Θ_R. We have not, however, addressed the effects of Ar addition on the amount of vibrational heating occurring in the system as there is not a sufficiently high population of vibrationally excited SiH for us to detect in our systems under the conditions used here.

V. Summary

We have studied the effects of argon dilution on the translational and rotational energy equilibration of SiH in both SiH_4/Ar and Si_2H_6/Ar plasmas using the IRIS technique. Within the investigated gas ratio range, the rotational temperature of SiH shows no dependence on the Ar dilution in both systems, which indicates that the SiH rotational energy has been thermalized. Ar dilution does, however, have different effects on the SiH translational temperatures in the two plasma systems, which is caused by different SiH_4 concentrations in the gas phase. The gas-phase SiH_4 concentrations in SiH_4/Ar plasmas are higher. Thus, in this system, there is no clear dependence of Θ_T on the Ar dilution, which indicates that the loss of SiH through reaction with SiH_4 in the gas phase is significant. The detected SiH radicals are likely nascent radicals formed in the direct electron impact dissociation of SiH_4. In contrast, $\Theta_T(SiH)$ in Si_2H_6/Ar plasmas decreases significantly as the fraction of Ar increases, which suggests that SiH radicals in the argon-diluted disilane plasma efficiently lose their kinetic energy through nonreactive collisions.

Acknowledgment. This work was supported by the National Science Foundation (NSF0137664).

References and Notes

(1) Kessels, W. M. M.; McCurdy, P. R.; Williams, K. L.; Barker, G. R.; Venturo, V. A.; Fisher, E. R. *J. Phys. Chem. B* **2002**, *106*, 2680.
(2) Ho, P.; Breiland, W. G.; Buss, R. J. *J. Chem. Phys.* **1989**, *91*, 2627.
(3) Longeway, P. A.; Weakliem, H. A.; Estes, R. D. *J. Phys. Chem.* **1984**, *88*, 3282.
(4) Hertl, M.; Jolly, J. *J. Phys. D*: *Appl. Phys.* **2000**, *33*, 381.
(5) Shirai, H.; Sakuma, Y.; Moriya, Y.; Fukai, C.; Ueyama, H. *Jpn. J. Appl. Phys., Part 1* **1999**, *38*, 6629.
(6) McCurdy, P. R.; Truitt, J. M.; Fisher, E. R. *J. Vac. Sci. Technol., A* **1999**, *17*, 2475.
(7) Kono, A.; Hirose, S.; Kinoshita, K.; Goto, T. *Jpn. J. Appl. Phys., Part 1* **1998**, *37*, 4588.
(8) Kono, A.; Koike, N.; Nomura, H.; Goto, T. *Jpn. J. Appl. Phys., Part 1* **1995**, *34*, 307.
(9) Kessels, W. M. M.; Hoefnagels, J. P. M.; Boogaarts, M. G. H.; Schram, D. C.; van de Sanden, M. C. M. *J. Appl. Phys.* **2001**, *89*, 2065.
(10) Shirafuji, T.; Tachibana, K.; Matsui, Y. *Jpn. J. Appl. Phys., Part 1* **1995**, *34*, 4239.
(11) Amorim, J.; Baravian, G.; Jolly, J. *J. Phys. D*: *Appl. Phys.* **2000**, *33*, R51.
(12) Kono, A.; Hirose, S.; Goto, T. *Jpn. J. Appl. Phys., Part 1* **1999**, *38*, 4389.
(13) Yamamoto, Y.; Suganuma, S.; Ito, M.; Hori, M.; Goto, T. *Jpn. J. Appl. Phys., Part 1* **1997**, *36*, 4664.
(14) Matsumi, Y.; Hayashi, T.; Yoshikawa, H.; Komiya, S. *J. Vac. Sci. Technol., A* **1986**, *4*, 1786.
(15) Stamou, S.; Mataras, D.; Rapakoulias, D. *J. Phys. D*: *Appl. Phys.* **1998**, *31*, 2513.
(16) Zhang, J.; Williams, K. L.; Fisher, E. R. *J. Phys. Chem. A* **2003**, *107*, 593597.
(17) McCurdy, P. R.; Butoi, C. I.; Williams, K. L.; Fisher, E. R. *J. Phys. Chem. B* **1999**, *103*, 6919.
(18) McCurdy, P. R.; Venturo, V. A.; Fisher, E. R. *Chem. Phys. Lett.* **1997**, *274*, 120.
(19) McCurdy, P. R.; Bogart, K. H. A.; Dalleska, N. F.; Fisher, E. R. *Rev. Sci. Instrum.* **1997**, *68*, 1684.
(20) Bogart, K. H. A.; Cushing, J. P.; Fisher, E. R. *J. Phys. Chem. B* **1997**, *101*, 10016.
(21) Fisher, E. R.; Ho, P.; Breiland, W. G.; Buss, R. J. *J. Phys. Chem.* **1993**, *97*, 10287.
(22) Zhang, J.; Fisher, E. R. *J. Phys. Chem. B* **2004**, *108*, 9821.
(23) Buss, R. J.; Ho, P. *IEEE Trans. Plasma Sci.* **1996**, *24*, 79.
(24) Bogart, K. H. A.; Cushing, J. P.; Fisher, E. R. *Chem. Phys. Lett.* **1997**, *267*, 377.
(25) Patterson, G. N. *Introduction to the Kinetic Theory of Gas Flows*; University of Toronto Press: Toronto, 1971.
(26) Bauer, W.; Becker, K. H.; Duren, R.; Hubrich, C.; Meuser, R. *Chem. Phys. Lett.* **1984**, *108*, 560.
(27) Luque, J.; Crosley, D. R. "LIFBASE: Database and spectral simulation (version 1.5)," SRI International, 1999.
(28) Nomura, H.; Kono, A.; Goto, T. *Jpn. J. Appl. Phys., Part 1* **1994**, *33*, 4165.
(29) Gallagher, A.; Howling, A. A.; Hollenstein, C. *J. Appl. Phys.* **2002**, *91*, 5571.
(30) Doyle, J. R.; Doughty, D. A.; Gallagher, A. *J. Appl. Phys.* **1992**, *71*, 4727.
(31) Schmitt, J. P. M.; Gressier, P.; Krishnan, M.; de Rosny, G.; Perrin, J. *J. Chem. Phys.* **1984**, *84*, 281.
(32) Perrin, J.; Delafosse, E. *J. Phys. D*: *Appl. Phys.* **1980**, *13*, 759.
(33) Nomura, H.; Akimoto, K.; Kono, A.; Goto, T. *J. Phys. D*: *Appl. Phys.* **1995**, *28*, 1977.
(34) Tanaka, T.; Hiramatsu, M.; Nawata, M.; Kono, A.; Goto, T. *J. Phys. D*: *Appl. Phys.* **1994**, *27*, 1660.
(35) Zhou, J.; Ayers, R.; Adams, E.; Martin, I. T.; Liu, D.; Fisher, E. R. *Plasma Sources Sci. Technol.*, manuscript in preparation.